A PRESSURE-SENSING SMART STENT COMPATIBLE WITH ANGIOPLASTY PROCEDURE AND ITS *IN VIVO* TESTING

Xing Chen[1], Babak Assadsangabi[1], Daniel Brox[1], York Hsiang[2], and Kenichi Takahata[1]
[1]Department of Electrical and Computer Engineering, University of British Columbia, Vancouver, B.C., Canada
[2]Department of Surgery, University of British Columbia, Vancouver, B.C., Canada

ABSTRACT

This study advances the technology for "smart" antenna stents integrated with micro pressure sensors, targeting at providing a non-invasive and rapid diagnosis of stenting-induced complications in a wireless manner. The smart stent device is developed via considering both engineering and clinical practicality with enhanced electromechanical performance over reported counterparts. The fabricated prototypes are assembled on balloon catheters while withstanding crimping forces well greater than 100 N, and show wireless local pressure sensing with a resolution of 12.4 mmHg upon balloon expansion. Using a swine model, the device is successfully operated to demonstrate wireless detection of blood clot formation, as well as real-time tracking of blood pressure change over a mean arterial pressure of 108 mmHg.

INTRODUCTION

Atherosclerosis, or hardening of the arteries, is the pathologic condition of plaque buildup on the arterial wall, progressively narrowing the arteries to obstruct blood flow. One of the most common treatments of this problem is stenting. Stents are tubular metal implants that are permanently placed in narrowed arteries to physically open and scaffold the vessels to restore blood flow [1]. The presence of a metallic stent within an artery, however, can cause inflammation that may lead to re-narrowing, or restenosis, of the artery. The likelihood of in-stent restenosis can be as high as 50% among stented patients [2]. Drug-eluting stents are currently used to limit restenosis; however, the newer generation stents have an increased risk of late thrombosis and resultant acute heart attacks over time [3]. The two primary methods presently used to clinically identify in-stent restenosis, duplex ultrasound and angiography, are usually not directed to patients until they experience chest pain or other indicative symptoms, and their clinical assessments can only be carried out by hospitalization with high cost [4].

In order to offer a non-invasive, rapid and easily-accessible diagnostic means, "smart" stents with self-sensing and communication ability achieved via integration of micro-electro-mechanical systems (MEMS), microelectronics, and antenna functions have been studied to enable early detection of the restenosis problem [5-7]. Unfortunately, these attempts have not reached successful *in vivo* demonstrations of their targeted functions. This outcome may be related to the following factors. First, proposed designs only considered engineering aspects without addressing their utility in real clinical settings, such as the compatibility with standard angioplasty and stenting procedures [5, 6]. Another related issue is chip packaging and integration on stents, which has mostly used adhesives or other methods that are not reliable [7, 8] and can easily fail in both the harsh mechanical steps involved during the stenting procedure (i.e., stent crimping, insertion, and expansion) and over the long term *in vivo*.

The primary focus of this work with respect to its engineering aspect is to build a smart stent integrated with a MEMS capacitive pressure sensor that simultaneously offers a high-performance wireless sensing function and a mechanical robustness required as a stent. Toward this end, microwelding-based packaging is used for the MEMS sensor integration on stents [9]. From a physiological and clinical perspective, the device is constructed and encapsulated with biocompatible materials, while being designed to comply with a standard assembly for the catheterization procedure enabled with high mechanical robustness of the developed device.

WORKING PRINCIPLE

Figure 1 illustrates a representative scenario of how the smart stent is implanted to treat a narrowed artery due to plaque deposition and to detect early signs of in-stent restenosis. Following a procedure same as standard percutaneous coronary intervention (PCI), a pressure-sensor-integrated stent is firmly crimped onto a balloon catheter (Figure 1(a)) and guided to the site of stenosis through a sheath; the balloon is then inflated to expand and deploy the stent, thereby widening the narrowed blood channel and restore the normal blood flow. Deflating and retracting the balloon catheter leaves the stent implanted permanently to scaffold the artery together with the integrated sensor (Figure 1(b)). The stent in this system is designed to function not only as a typical mechanical scaffold but also as an electrical inductor or antenna [10]. Using a capacitive type of MEMS pressure sensor that works as a variable capacitor over pressure, a combination of the stent and the sensor forms a passive inductor-

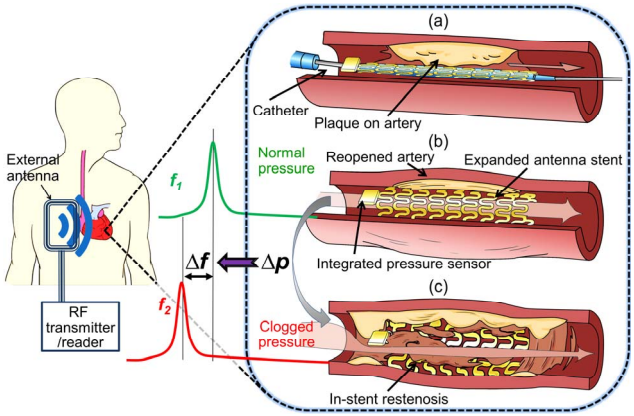

Figure 1: Conceptual schematic of the smart stent device and its implantation, wirelessly providing in-stent blood pressure signal for early detection of restenosis.

capacitor (*LC*) tank, whose resonant frequency represents the on-site condition of surrounding blood pressure, which may be interrogated using a handheld wireless reader with an external antenna by establishing inductive coupling with the inductive stent. Upon the onset of in-stent restenosis, in which condition excess tissue and plaque builds up on the inner walls of the stent to obstruct blood flow, hemodynamics and local pressure distribution around the stent changes (Figure 1(c)), and accordingly, the resonant frequency shifts away from its original value as a sign of in-stent restenosis. This change provides critical information that guides the patient to proceed to in-depth examination and further treatments at early stages.

DESIGN AND FABRICATION

The targeted stent device is comprised of two main components, an inductive stent and a capacitive pressure microsensor (Figure 2(a)). The stent is designed to have an overall helical pattern, acting as not only a mechanical scaffold same as conventional stents, but also an electrical inductor that serves as radiofrequency antennas [10]. The inductive stents with a length of 30 mm are created to have 23 helical turns with an inductance of 268 nH (at 10 MHz) in the pre-expansion state. Two tab-like structures (0.6×2.0 mm^2) are designed at both ends of the stent to be used as the platforms for sensor integration. The antenna stents are laser-micromachined out of medical-grade (type 316L) stainless-steel tubing with an inner diameter of 1.8 mm and a wall thickness of 100 µm (Figure 2(a)). The stents are electroplated with gold for 15-20 µm thickness to decrease the series resistance of the stent and thus enhance its Q factor. The DC resistances of the antenna stents were measured to decrease by 15× (from 22.5 Ω to 1.5 Ω on average) after gold plating. The stents are passivated by a 20-µm-thick Parylene C layer to make their surfaces electrically isolated and biocompatible.

The MEMS capacitive pressure sensor used for smart stent construction is also custom designed and microfabricated (Figure 2(a)). This gauge pressure sensor is comprised of a microchip of the same stainless steel as the antenna stent, which is used as the sensor's substrate as

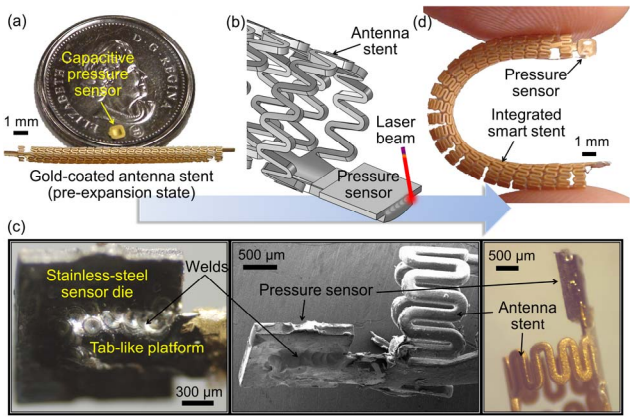

Figure 2: (a) Fabricated pressure sensor chip (on Canadian quarter) and 30-mm inductive stent, (b) laser microwelding process joining a sensor chip onto the stent, (c) close-up photos (left and right) and SEM image (middle) showing microwelded joint between the chip and the stent, and (d) finalized device integrated by laser microwelding.

well as the fixed capacitive electrode, and a gold-polyimide multilayered diaphragm serving as the other electrode that is movable. The sensor chip is designed to be thin (200 µm) with a small footprint (1.5×1.5 mm^2) to minimize blood flow turbulence, and entirely made of biocompatible materials (titanium and SiO_2 besides the above noted materials). Micro-electro-discharge machining is used to pattern the stainless-steel chip with the reference cavity, which is sealed at atmospheric pressure with the flexible diaphragm via thermal bonding; detailed process of sensor fabrication can be found in [9].

For sensor integration with the inductive stent, this study uses laser microwelding, instead of using conductive epoxy as reported previously [8], to exploit both engineering and physiologic sides of the benefits. For example, microwelded bonds were shown to provide 2× larger shear strength and 6× higher electrical conductance compared with those of conductive epoxy [9]. The high conductance contributes to raising the Q factor of the *LC* tank, i.e., the sensor-stent combination. The microwelded bonds also offer high resistance against corrosion and demonstrated a long-term reliability within the human body [11]. The microwelding process is conducted using a commercial Nd:YAG fiber-laser system (FiberStar Workstation 7600, LaserStar Technologies Co., USA). A focused laser beam with a spot diameter down to ~25 µm available with the system enables micro-scale and direct (no filler) welding at the interface between the sensor die and the stent. To minimize the thermal impact to the sensor, the single pulse mode is used instead of the seam mode (the peak power and pulse duration of the laser is chosen to be 130 W and 0.5 ms from a preliminary study [9]). A three-axis micromanipulator is used to precisely position the sensor chip with respect to the tab platform of the stent (the Parylene film on the tab is manually removed in advance), followed by shooting the laser on their interface region at multiple spots to weld the sensor onto the stent (Figure 2 (b)). As evident from Figure 2(c), this process is effective to fuse micro regions of the sensor die and stent together to create continuous, robust bond with low profile. The resultant device potentially allows smooth stenting operations, preventing its mechanical failure while minimizing disturbance of blood flow by the presence of sensor upon device implantation.

The *LC* circuit is completed by electrically bridging between the electrode of sensor's diaphragm and the other side of the stent's tab using a thin (80-µm-thick) copper wire. Finally, another layer of Parylene C (2-µm thickness) is deposited to ensure both electrical insulation and biocompatibility on all surfaces of the integrated device, completing the fabrication process (Figure 2(d)).

RESULTS AND DISCUSSION

Compatibility with Standard Angioplasty Procedure

To bring the smart stent technology into practice, it is essential for the device to meet clinical standard used for commercial products. In light of this, the compatibility of fabricated prototypes with a PCI procedure was assessed through bench tests. To start with, an integrated device was mounted and aligned onto the balloon region of commercial balloon catheters (e.g., Low Profile PTA

Balloon Dilatation Catheter, Cook Medical Inc., IN, USA), and a handheld stent crimper (HH100 SS, Machine Solution Inc., AZ, USA) was used to exert radial compression force to the stent device (Figure 3(a)) to crimp it onto the balloon by reducing its initial diameter. The radial forces in the order of 100 N was applied to achieve tight crimping, a critically important factor for proper and successful device delivery. As performed in a PCI process, the stent-balloon assembly was forced to open a tightly closed hemostasis valve at the end of a sheath introducer (Check-Flo® Performer Extra Large Introducer, Cook Medical Inc., IN, USA) in order to pass through the sheath and reach an artery. The assembly was verified to easily pass through the sheath introducer (Figure 3(b)) with no apparent interference to the device – this was achieved through two main advantages of the adopted microwelding approach to sensor integration, i.e., high mechanical robustness of the bond against shear stress caused by pushing into the hemostasis valve, and the small footprint and low profile of the resultant device that enabled smooth insertion with minimized guiding resistance. Passing through the sheath-valve tube, the device was delivered into a silicone-based artificial artery (6-mm diameter, Dynatek Labs, MO, USA) for the final deployment. Deionized water was injected into the balloon with an inflation tool to fully inflate the balloon with pressure up to 16 atm (Figure 3(c)). X-ray imaging of the device deployed and implanted inside a pig model (Figure 3(d), performed in one of *in vivo* tests) demonstrates high radiopacity of the device brought by both the gold coating on the stent surfaces and the gold layer of the sensor diaphragm.

The prototypes that experienced all the assembly and delivery steps described above were tested to show ~80% success rate with no failure in both mechanical and electrical functions. This was not the case for those with conductive epoxy, which indeed showed frequent breakaway of the sensors from the stents while experiencing these steps. The results indicate that the developed smart stent device is promising to be compatible with the standard PCI procedure and practice, potentially in a level equivalent to commercial stents through further design optimization.

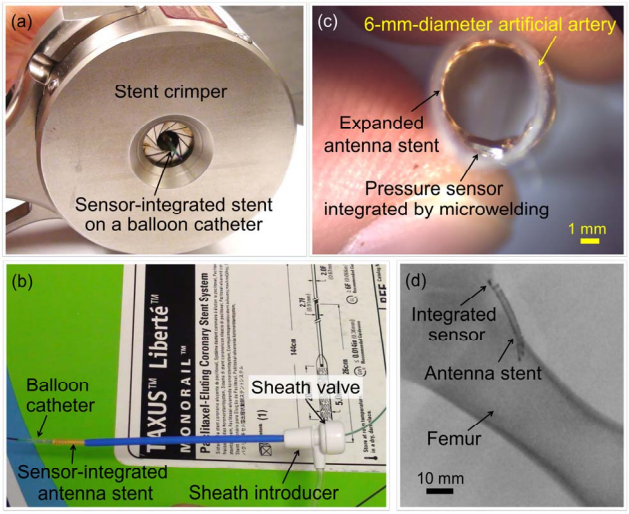

Figure 3: Testing through standard angioplasty/stenting procedure for the developed smart stent: (a) Crimping on balloon catheter; (b) guiding through sheath introducer; (c) expansion in artificial artery; (d) X-ray image showing radiopacity of the device implanted in a swine model.

In Vitro Electrical and Wireless Tests

The electrical and sensor behavior of the prototypes were wirelessly characterized using an external antenna (inductively coupled with the antenna stents) connected to an impedance analyzer (4396B, Agilent Technologies Co., CA, USA). Figure 4(a) shows the measured impedance phase dips led by two devices, one integrated with microwelding, and the other with conductive adhesive, expanded to the same diameter. Prior to this test, their series resistances were also measured. As expected, the former device exhibited a lower resistance and a higher Q factor than those of the latter device (4.6 Ω vs. 8 Ω, and 39 vs. 21, respectively) due the electrical merit offered by microwelding. A sensor-microwelded device deployed in a 6-mm-diameter vascular graft (GORE-TEX® Stretch Vascular Graft, W. L. Gore & Associates, Inc., AZ, USA) was coupled with a flow loop, and the device's response in the reflection phase dip to varying intraluminal pressures produced in water flow was measured (Figure 4(b)). The shifts of the resonant frequency were clearly resolved towards lower values (due to increase of sensor's capacitance) as pressure was increased with an increment of 12.4 mmHg. A total frequency shift of 200 KHz was observed over the full pressure change of 62 mmHg.

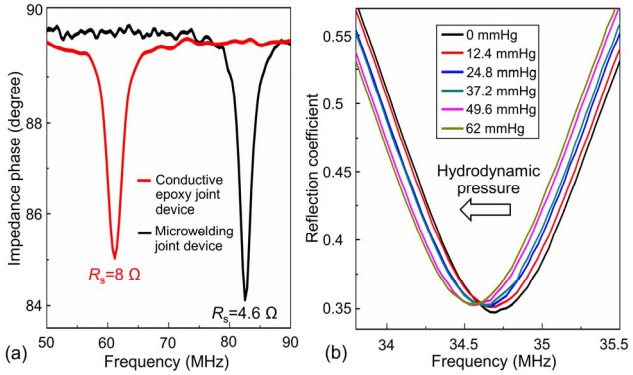

Figure 4: (a) Impedance phase dips of two expanded devices with sensors integrated by microwelding and conductive epoxy, and (b) resonant frequency shifts of microwelded device with varying pressure in water flow.

In Vivo Tests

The developed prototypes were tested with a swine model under ethics protocol #A11-0067 of the University of British Columbia. Given the small size of model's blood vessels, a bypass surgical model was created using the device-deployed vascular grafts. In the first test, a 5-mm-diameter graft that contained two expanded devices, one functional, and the other as a control without pressure response, was anastomosed into a ligated superficial left carotid artery. A catheter that linked a commercial pressure transducer was inserted into the artery (Figure 5) and positioned in proximity to the graft at its upstream for reference pressure reading. The repetitive stoppage of blood flow (performed as a preliminary test of device's pressure response) led to a blood clot formed inside the graft, creating a scenario similar to in-stent restenosis. The

comparison of the reflection dip spectrums observed in an external antenna before and after the clot formation (Figure 6(a)) showed no frequency shift with the control device, whereas that of the functional device exhibited a clear shift (~+380 KHz) upon clotting. In another test with a new graft-device combination (6-mm diameter) conducted with the same swine, blood pressure was systemically raised by administrating dobutamine, a vasoconstrictor drug. As the drug was delivered, the swine's blood pressure increased to 138/94 mmHg (a mean arterial pressure (MAP) of 108 mmHg) as read by the reference transducer. The device in the graft, wirelessly interrogated via the external antenna, responded to this pressure increase, as a consistent decrease of resonant frequency by ~3.5% from its base value (of 27.96 MHz, at a MAP of 59 mmHg; Figure 6(b)). Finally, the pig was euthanized, and the blood pressure gradually decreased towards 0 mmHg; the device responded to this pressure drop as well, with corresponding rise of its resonant frequency as also shown in Figure 6(b). This test verified the effectiveness of the developed prototype for real-time tracking of local blood pressure, over a blood pressure range close to that of human.

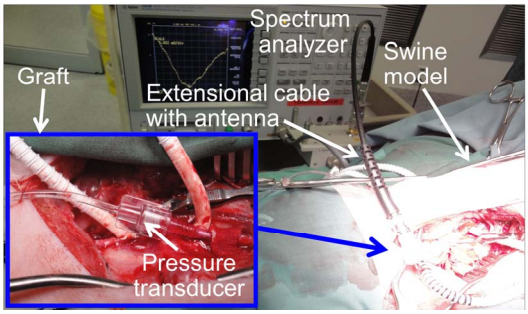

Figure 5: Measurement set-up used for animal testing.

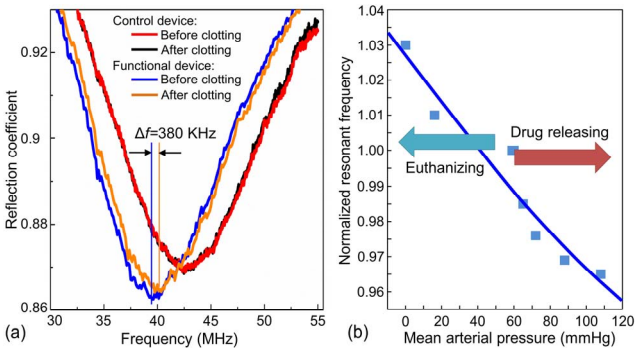

Figure 6: (a) Wirelessly measured frequency response of functional and control stent devices to blood clot formation in the graft, and (b) normalized resonant frequency shifts wirelessly recorded with the swine model showing real-time tracking for a MAP range over 100 mmHg.

CONCLUSION

A smart stent device integrated with a MEMS-based capacitive pressure sensor has been investigated and developed to achieve an enhanced electromechanical performance required for real surgical preparation and procedure. The effectiveness of the adopted approach to the design and fabrication of the antenna stent and pressure sensor as well as their packaging based on microwelding was experimentally proved through *in vitro* and *in vivo* studies with promising results. It is evident from the results that the microwelding-based method for sensor-stent integration significantly raised the practicality of the stent in both mechanical and electrical functions of the device, leading to the demonstration of continuous wireless tracking of local blood pressure with an animal model. Further device optimization will be conducted to raise the sensing ability as well as the reliability of the device.

ACKNOWLEDGMENTS

This work was partially supported by the Canadian Institutes of Health Research, the Natural Sciences and Engineering Research Council of Canada, the Canada Foundation for Innovation, the British Columbia Knowledge Development Fund, and Canadian Microelectronics Corporation. K. Takahata is supported by the Canada Research Chairs program.

REFERENCES

[1] H.W. Roberts, S.W. Redding, "Coronary artery stents: review and patient-management recommendations," *J. Am. Dent. Assoc.*, 131(6), pp. 797-801, 2000.

[2] H.C. Lowe, S.N. Oesterle, L.M. Khachigian, "Coronary in-stent restenosis: current status and future strategies," *J. Am. Coll. Cardiol.*, 39(2), 183-93, 2002.

[3] M. Joner, A.V. Finn et al., "Pathology of drug-eluting stents in humans: delayed healing and late thrombotic risk," *J. Am. Coll. Cardiol.*, 48(1), 193-202, 2006.

[4] M.N. Gulari et al., "An implantable X-ray-based blood pressure microsensor for coronary in-stent restenosis surveillance and prevention," *J. Microelectromech. Syst.*, 24(1), pp. 50-61, 2015.

[5] K. Takahata, Y.B. Gianchandani, K.D. Wise, "Micromachined antenna stents and cuffs for monitoring intraluminal pressure and flow," *J. Microelectromech. Syst.*, 15(5), pp. 1289-98, 2006.

[6] E.Y. Chow, A.L. Chlebowski, S. Chakraborty et al., "Fully wireless implantable cardiovascular pressure monitor integrated with a medical stent," *IEEE Trans. Biomed. Eng.*, 57(6), pp. 1487-96, 2010.

[7] S.R. Green, R.S. Kwon et al., "*In vivo* and in situ evaluation of a wireless magnetoelastic sensor array for plastic biliary stent monitoring," *Biomed. Microdev.*, 15(3), pp. 509-19, 2013.

[8] X. Chen, D. Brox, B. Assadsangabi, Y. Hsiang, K. Takahata, "Intelligent telemetric stent for wireless monitoring of intravascular pressure and its *in vivo* testing," *Biomed. Microdev.*, 16(5), pp. 745-59, 2014.

[9] X. Chen, D. Brox, B. Assadsangabi, M.S. Mohamed Ali, K. Takahata, "A stainless-steel-based capacitive pressure sensor chip and its microwelding integration," *IEEE Transducers*, pp. 1081-4, 2015.

[10] A.R. Mohammadi, M.S. Mohamed Ali, D. Lappin, C. Schlosser, K. Takahata, "Inductive antenna stent: design, fabrication, and characterization," *J. Micromech. Microeng.*, 23(2), 025015, 2013.

[11] Y.H. Joung, "Development of implantable medical devices: from an engineering perspective," *Int. Neurourol. J.*, 17(3), pp 98-106, 2013.

CONTACT

*K. Takahata, tel: +1-604-827-4241; takahata@ece.ubc.ca